Characteristics of atmospheric turbulence in terms of background atmospheric parameters inferred using MST radar at Gadanki (13.5°N, 79.2°E)

Siddarth Shankar Das,[1] A. K. Ghosh,[2] K. Satheesan,[3] A. R. Jain,[4] and K. N. Uma[1]

[1] Indian mesosphere-stratosphere-troposphere (MST) radar is located at Gadanki (13.5°N, 79.2°E) in a tropical zone of India. In this region the background atmospheric parameters such as atmospheric winds, temperature, and humidity show a distinct change from monsoon to winter season. For example, the monsoon season is dominated by tropical easterly jet winds in the upper troposphere (i.e., 14–17 km), and the winter season is dominated by westerly winds with peak value at about 12–14 km. The basic wind patterns in the two seasons differ significantly, and this is expected to give rise to differences in the characteristics of atmospheric turbulence parameters in the two seasons. In this paper, various atmospheric turbulence parameters such as eddy dissipation rate (ε), eddy diffusivity (K_h), and horizontal scale length (l_0 and L_B) are obtained for the first time for the monsoon and winter seasons by using the available data sets from MST radar. An attempt is made to understand and explain the seasonal variability of these turbulence parameters in terms of the observed changes in the background atmospheric conditions.

1. Introduction

[2] It is well known that turbulence present in different regions of the atmosphere forms an important component of the atmospheric dynamics. Study of atmospheric turbulence is of interest to radar and aircraft engineers for the selection of radar wavelength and design of aircraft. This is also of considerable interest to the meteorologist for understanding the atmospheric dynamics, mixing, and pollutant dispersion, etc. Turbulence is also of important interest for understanding the general circulation of the atmosphere as it contributes to the dissipation of kinetic energy and enhances mixing of properties of flow such as momentum. The presence of turbulence in the atmosphere also determines the mixing and diffusion of various constituents such as ozone. Turbulence in the atmosphere is generated due to the strong vertical shear of the horizontal winds or due to the instability associated with atmospheric convection. These two mechanisms of turbulence generation are referred to as mechanical turbulence and thermal turbulence, respectively.

[3] Eddy dissipation rate (ε), eddy diffusivity (K_h), and horizontal inner and outer scale lengths (l_0 and L_B), respectively, are some of the basic turbulence parameters that define the strength and size of the atmospheric turbulence. The above atmospheric turbulence parameters depend on background atmospheric conditions such as temperature, wind speed, and vertical shear of horizontal winds. Since the atmospheric background parameters vary with seasons and latitudes, turbulence parameters also vary. Most of the measurements of turbulence characteristics are, however, confined to midlatitudes and high latitudes [*Gage et al.*, 1980; *Hocking*, 1983, 1985; *Nastrom et al.*, 1986; *Fukao et al.*, 1994; *Nastrom and Eaton*, 1997a, 1997b], and only a few measurements are available for tropical latitudes [*Sato and Woodman*, 1982; *Jain et al.*, 1995; *Rao et al.*, 1997, 2001; *Satheesan and Murthy*, 2002; *Ghosh et al.*, 2003]. The Indian tropical

Table 1. MST Radar Experimental Specification File Used for the Present Study

Parameter	Mode 1	Mode 2
Pulse width (μs)	16	16
Interpulse period (μs)	1000	1000
Coded/uncoded	coded using 16 baud biphase supplementary	coded using 16 baud biphase supplementary
Range resolution (m)	150	150
Number of beams	6 (E_{10y}, W_{10y}, Z_y, Z_x, $N10_x$, S_{10x})[a]	Z_x[a]
Number of coherent integrations	128	128
Number of FFT points	128	128
Nyquist frequency (Hz)	±4 (line of sight velocity v~±12 m/s)	±4 (line of sight velocity v~±12 m/s)
Doppler resolution (Hz)	0.06 (line of sight (∇v) ~ 0.18 m/s)	0.06 (line of sight (∇v) ~ 0.18 m/s)
Lowest range bin (km)	3.6	3.6
Highest range bin (km)	32	32
Incoherent integrations	1	1
Beam dwell time (s)	16	16
STC length (μs)	40	40
Number of scan cycles	8	120

[a]Here, E_{10y}, beam direction 10° east from the zenith in east–west plane; W_{10y}, beam direction 10° west from the zenith in east–west plane; Z_y, vertical beam direction formed using east–west plane; Z_x, vertical beam direction formed using north–south plane; N_{10x}, beam direction 10° north from the zenith in north–south plane; S_{10x}, beam direction 10° south from the zenith in north–south plane.

region shows a distinct seasonal variation in wind and associated vertical shear, and the year is divided into four seasons, namely, winter (December, January, and February), premonsoon (March, April, and May), monsoon (June, July, and August), and postmonsoon (September, October, and November) [*Ghosh et al.*, 2001; *Rao et al.*, 2008]. Out of these four seasons, monsoon and winter seasons are totally different in their characteristics. During monsoon season, strong tropical easterly jet (TEJ) winds are observed at the height region of 14–17 km just near the mean tropical tropopause [*Das et al.*, 2008] with a peak value of 45–50 m s^{-1} [*Sathiyamoorthy*, 2005]. These jet winds are associated with the strong vertical shears above the peak wind height. During winter season the winds are relatively weaker and are dominated by the westerly winds, with peak values of 10–14 m s^{-1}, which appear at the height range of 10–14 km. Thus, there is a sharp contrast in the observed winds during winter and monsoon seasons.

[4] In this paper an attempt is made for the first time to determine the height profiles of various turbulence parameters such as ε, K_h, l_0, and L_B and to understand the changes in their characteristics from monsoon to winter season, in terms of background atmospheric conditions such as horizontal winds, associated vertical shears, and temperature.

2. Experimental Details and Data Analysis

[5] The National Atmospheric Research Laboratory (NARL) at Gadanki (13.5°N, 79.2°E), India, operates a mesosphere-stratosphere-troposphere (MST) radar, which is a Doppler radar at a frequency of 53 MHz and peak power aperture product of 3×10^{10} W m^{-2}. The antenna consists of a 32 × 32 array of 3 element Yagi aerials with covering a geometric area of 130 × 130 m^2. The radiation pattern of radar has 3° beam width with gain of 36 dB and first side lobe level of –20 dB. A detailed description of this radar is given by *Jain et al.* [1994] and *Rao et al.* [1995]. A detailed experimental specification file is given in Table 1.

[6] For the present study, two intensive campaigns carried out at Gadanki were used. The main themes of the campaigns were to study the various aspects of atmospheric dynamical processes associated with atmospheric convection, turbulence, waves, tides and tropopause dynamics. The first campaign (campaign 1) was carried out from 19 July to 14 August 1999, which is Indian summer monsoon period, and the second campaign (campaign 2) was from 19 January to 10 February 1999, which is the winter period. During campaign 1, everyday the radar was operated in two modes. In the first mode (see Table 1, mode 1) the radar was operated to obtain the three-dimensional wind fields (zonal, meridional, and vertical) between 1645 and 1730 IST (IST = GMT + 5:30 h), and in the second mode (see Table 1, mode 2) the radar was operated continuously between 1730 and 1930 IST in vertical beam mode. The second mode radar observations were used to collect the vertical beam echo power and vertical wind velocity. Along with radar observations, simultaneous in situ measurements were also carried out by launching radiosonde everyday at 1600 IST (IST = GMT + 05:30 h) for campaign 1. These radiosondes are of standard design developed by the

Table 2. Details of Data Used for the Present Study

Campaign	Period/Date of Observation	Mode of Operation	System Operated
1	19 Jul to 14 Aug 1999	Mode 1/Mode 2	MST radar and radiosonde flight
2	19 Jan to 10 Feb 1999	Mode 1/Mode 2	MST radar

India Meteorological Department (IMD) [*Jain et al.*, 2006]. Radiosonde measurements of pressure, temperature, and humidity data are obtained for every 1 min interval corresponding to a vertical height interval of ~300 m. The radiosonde reached an altitude of about 30 km in about 1 h 40 min from the time of launch. The radiosonde data are interpolated using linear interpolation at the height interval of 150 m to match the height levels of measurements by the two instruments. The atmospheric stability parameter (N^2) and vertical shear of horizontal wind ($\partial U_h/\partial z$) are computed for each radar range gate (150 m) with a vertical resolution of 300 m. Thus, the effective height resolution is ~150 m. Similarly, in campaign 2, the radar is also operated in both mode 1 and mode 2. For both of the two campaigns the three-dimensional winds are averaged over 30 min from ~1645 to 1715 IST. The continuous vertical velocity measurements for 2 h from ~1730 to 1930 IST are considered for the present analysis to estimate Brunt-Vaisala frequency (N). The details of the data used for the present study are given in Table 2.

3. Methods of Determining Atmospheric Turbulence Parameters

[7] Different methods of determining atmospheric turbulence parameters have been discussed [*Hocking*, 1985; *Nastrom et al.*, 1986; *Rao et al.*, 1997, 2001; *Satheesan and Murthy*, 2002; *Ghosh et al.*, 2003]. There are three methods for determining turbulence parameters using radar spectral parameters, namely, (1) power, (2) spectral width, and (3) variance methods. Actually, there are two methods that make use of observed spectral width, namely, spectral width method 1 and spectral width method 2. In spectral width method 1, Brunt-Vaisala frequency N is required for estimation the turbulence parameters, which are normally derived from the in situ measurements of temperature. In spectral width method 2, only the antenna characteristics are used and no temperature measurements are required. Estimation of turbulence parameters using spectral width method 2 may not be possible to find accurately at the height where wind shear is high [*Cohn*, 1995]. *Hocking* [1996] and *Nastrom and Eaton* [1997a] reported that the spectral width method 2 is appropriate only in the lower atmosphere below 5 km, whereas width method 1 is more appropriate at higher altitudes. So, in the present study, spectral width method 1 is used for estimating turbulence parameters like (1) eddy dissipation rate (ε), (2) eddy diffusivity (K_h), (3) buoyancy scale size (L_B), and (4) the minimum scale size (l_0). The spectral width method makes use of the observed radar received signal half spectral width to determine ε [*Cunnold*, 1975; *Sato and Woodman*, 1982; *Hocking*, 1983, 1985; *Fukao et al.*, 1994; *Jain et al.*, 1995; *Nastrom and Eaton*, 1997a, 1997b; *Rao et al.*, 1997, 2001; *Ghosh et al.*, 2003]. It is to be noted that, spectral width is estimated using oblique beam instead of vertical beam as MST radar (53 MHz) vertical beam is very sensitive to specular reflections. Thus, the spectral width is estimated from the oblique beam as oblique beam is largely free from Fresnel scattering/reflection [*Rotteger and Larsen*, 1990]. The effect of specular reflections is free beyond 10° oblique beam [*Gage and Balsley*, 1980]. However, the observed radar signal spectral width ($\sigma_{1/2\mathrm{obs}}$) in the oblique beam consist of real spectral width ($\sigma_{1/2}$) due to backscattering from refractive index irregularities associated with atmospheric turbulence along with (1) beam broadening due to finite beam volume ($\sigma_{1/2\mathrm{beam}}$), (2) broadening due to wind shear ($\sigma_{1/2\mathrm{shear}}$), and (3) also contamination due to transience effect ($\sigma_{1/2\mathrm{transit}}$) [*Atlas et al.*, 1969; *Sato and Woodman*, 1982; *Hocking*, 1983, 1985, 1986, 1996; *Hocking and Lawry*, 1989; *Fukao et al.*, 1994; *Jain et al.*, 1995; *Rao et al.*, 1997; *Nastrom and Eaton*, 1997a, 1997b; *Ghosh et al.*, 2003]. Another effect by which spectral width may be contaminated is due to the gravity waves ($\sigma_{1/2wave}$) [*Murphy et al.*, 1994; *Nastrom and Eaton*, 1997a]. That is the measured signal spectral width $\sigma_{1/2\mathrm{obs}}$ may be contaminated by nonturbulent factors and thus, the broadening corrected spectral width $\sigma_{1/2}$ is given by:

$$\left(\sigma_{1/2}\right)^2 = \left(\sigma_{1/2obs}\right)^2 - \left(\sigma_{1/2beams}\right)^2 - \left(\sigma_{1/2shear}\right)^2 - \left(\sigma_{1/2trans}\right)^2 - \left(\sigma_{1/2wave}\right)^2 \quad (1)$$

The contribution of the spectral width due to beam and shear broadening are given by [*Hocking*, 1983, 1985, 1986; *Ghosh et al.*, 2003]:

$$\sigma_{1/2beam} = \delta_{1/2}\left|\overline{U_h}\right| \quad (2)$$

$$\sigma_{1/2shear} = \frac{1}{2}\left|\frac{\overline{\partial U_h}}{\partial z}\right|\Delta z \sin\chi \quad (3)$$

where U_h and $|\overline{\frac{\partial U_h}{\partial z}}|$ are the horizontal wind speed and vertical shear of horizontal wind respectively with height (z). For Gadanki MST radar, the half power half width ($\delta_{1/2}$) of the two way radar beam (1.1°) is 0.0019 rad. Before calculating the wind shear, the wind data are also averaged over ~30 min to remove the high-frequency fluctuation.

[8] It is to be noted that in the present analysis the number of incoherent integration of the spectrum is unity (see Table 1), and the beam dwell time is estimated to be 16 s. Thus, the spectral width contamination due to transience effect ($\sigma_{1/2\text{transit}}$) is minimal and can be neglected for the present analysis. However, the effects of gravity wave on spectral broadening is estimated by using hourly mean standard deviation of vertical velocity (mode 2 experiment) as described by *Nastrom and Eaton* [1997a]. The estimated $(\sigma_{1/2\text{wave}})^2$ is again reduced by a factor 3/4 to account for a circular shape of MST radar beam pattern instead of square [*Nastrom and Eaton*, 1997a]. In the present analysis, $(\sigma_{1/2\text{wave}})^2$ is found to be relatively very small compared to the other correction factors and thus, the effect of gravity wave is neglected. The details of the spectral width correction can also be found elsewhere [e.g., *Hocking*, 1983, 1985, 1986; *Murphy et al.*, 1994; *Nastrom and Eaton*, 1997a; *Ghosh et al.*, 2003, and references therein].

3.1. Energy Dissipation Rate

[9] Energy dissipation rate is an important characteristic of atmospheric turbulence and it represents the amount of turbulence energy converted into heat of the medium by viscous forces per unit mass per unit time. The parameter ε is related to mean square fluctuations of velocity of the medium and the half power half spectral width of the received backscattered signal [*Weinstock*, 1981; *Hocking*, 1983, 1985; *Fukao et al.*, 1994; *Jain et al.*, 1995; *Nastrom and Eaton*, 1997a] by equation

$$\varepsilon = 0.49\overline{V^2}N = 0.33\sigma_{1/2}^2 N \tag{4}$$

It is worth noting that $\sigma_{1/2}$ is the half power half spectral width of the received signal spectra after correction for broadening effects as mentioned above.

3.2. Vertical Eddy Diffusivity

[10] The vertical eddy diffusivity K_h is defined by the kinematic heat flux and vertical gradient of the mean potential temperature, i.e.,

$$K_h \frac{\partial \theta}{\partial z} = -\overline{\theta' w'} \tag{5}$$

where w is the vertical velocity, θ is potential temperature, and the over bar and the prime denote the mean field and the perturbations, respectively.

[11] From the consideration of energy budget of the turbulence and the definition of the static stability parameter (N^2) it can be shown [*Fukao et al.*, 1994] that

$$K_h = \frac{\beta\varepsilon}{N^2}, \text{ where } \beta = \frac{R_f}{1 - R_f} \tag{6}$$

where R_f is the flux Richardson number. It should be noted that the above expression gives a local value of K_h for locally homogeneous turbulence (say for each radar volume cell).

[12] *Lilly et al.* [1974] used a value of 0.25 for R_f and obtained $\beta = 1/3 = 0.33$. This value of β is also consistent with the generalized formulation as given by *Weinstock* [1981] where the dominant turbulence scale is slightly smaller than the buoyancy scale. Equations (4), (5), and (6) yield

$$K_h = \sim 0.33\varepsilon N^{-2} \text{ or } K \sim 0.1\sigma_{1/2}^2 N^{-1} \tag{7}$$

3.3. Scale Size of Turbulence

[13] The inner scale and buoyancy scale size are important for the discussion of turbulence. The inner scale size of turbulence l_0 is estimated using the relationship

$$l_0 = 7.4\eta \tag{8}$$

where η is the Kolmogorov microscale.

$$\eta = \left(\frac{\upsilon^3}{\varepsilon}\right)^{\frac{1}{4}} \tag{9}$$

and

$$\upsilon = \frac{2.0 \times 10^{-5}}{\rho} \tag{10}$$

where υ, ε and ρ are the kinematic viscosity, eddy dissipation rate and the atmospheric density, respectively. Atmospheric density for determination of η and l_0 is taken from the model by *Sasi and Sen Gupta* [1986], which is a representative model for Indian tropical region.

[14] The buoyancy scale L_B determines the transition scale lengths between the inertial and buoyancy range and the same is given by [*Weinstock*, 1978; *Hocking*, 1985; *Jain et al.*, 1995]

$$L_B = \frac{2\pi}{0.62}\varepsilon^{1/2}N^{-3/2} \tag{11}$$

It should be mentioned here that equation (8) is applicable only to shear generated turbulence in statically

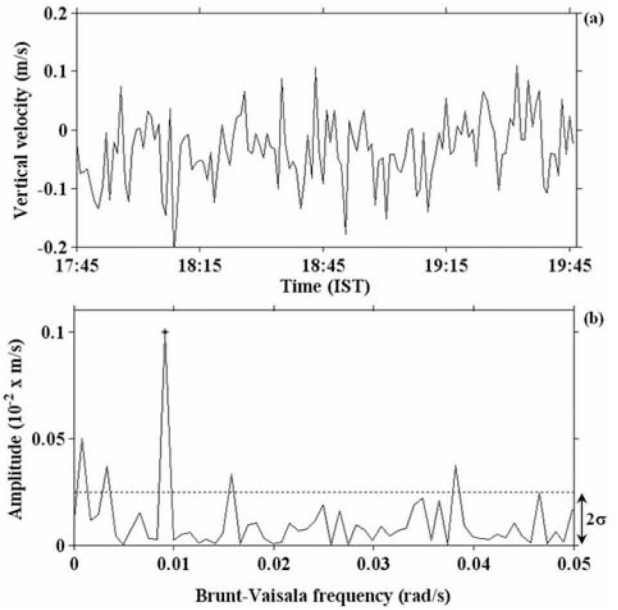

Figure 1. (a) Time series of vertical velocity at 8 km and (b) its corresponding spectrum on 21 July 1999. The star in the spectrum indicates the Brunt-Vaisala frequency (N), and the dotted line is twice the standard deviation (2σ), above which the peak is significant.

stable atmosphere. For convective turbulence, $N^2 < 0$ and therefore above equation would not be meaningful.

4. Method of Determining Stability Parameter N^2 Using MST Radar

[15] It is a well known fact that MST radar is a unique instrument to provide direct high resolutions (height and time) measurement of vertical velocity [*Rao et al.*, 1995, and references therein]. Though the magnitude of the vertical velocity in the troposphere and stratosphere is very low of the order of a few centimeters during clear-air conditions, it shows very high variability [*Uma and Rao*, 2009]. The peak corresponding to the spectrum of vertical velocity fluctuation indicates Brunt-Vaisala frequency, which have a typical characteristic of steep and slow decrease in the high and low frequency side, respectively. The typical vertical velocity fluctuation and its corresponding spectrum at 8 km are shown in Figures 1a and 1b, respectively. The star in the spectrum indicates the Brunt-Vaisala frequency N, and the dotted line is twice the standard deviation (2σ), above which the peak is significant. Similarly, the Brunt-Vaisala frequency is identified for each height to generate height profile. It is to be noted that the stability parameter can only be estimated during clear air, i.e., nonconvective day. Here the nonconvective day means the vertical velocity should be within ±1.0 m/s [*Uma and Rao*, 2009]. Thus for the present study, only nonconvective days are considered. The detailed method for the estimation of Brunt-Vaisala frequency from MST radar can be found in the works of *Rotteger* [1986] and *Revathy et al.* [1996].

[16] Figure 2 (left) shows the typical profile of N^2 derived from MST radar (solid line) and simultaneous radiosonde observation at Gadanki on 24 and 28 July 1999. It can be seen from Figure 2 that the height profile of N^2 derived from MST radar and radiosonde show comparable good agreement. Using N^2, the atmospheric temperature (T) can be estimated by using the relationship

$$N^2 = \frac{g}{T}\left[\frac{dT}{dz} + \Gamma\right] \tag{12}$$

where g, and Γ are acceleration due to gravity and adiabatic lapse rate, respectively [*Revathy et al.*, 1996]. Figure 2 (right) shows the typical profile of atmospheric temperature derived from MST radar (solid line) and simultaneous radiosonde observation at Gadanki on 24 and 28 July 1999, which show good comparison. The horizontal arrows indicate the corresponding cold point tropopause height. This shows the potential of MST radar to derived Brunt-Vaisala frequency and atmospheric temperature in clear air condition. The error in the estimation of Brunt-Vaisala frequency and atmospheric temperature derived form MST radar vertical velocity measurement is presented by *Revathy et al.* [1998]. Authors have found that the standard deviation of N = 0.0018 for 60 min of radar observations. Thus, the standard deviation of temperature is between 0.29 and 1.1 K with 300 m height resolution. However, for the present study, N^2 derived from MST radar are directly used for the estimation of turbulence parameters.

5. Observational Results

5.1. Height Profiles of Temperature and Stability Parameter N^2 During Monsoon and Winter Seasons

[17] Figure 3 shows the height profiles of Brunt-Vaisala frequency and temperature for two days of monsoon and winter seasons using MST radar observations. Height profile of N^2 and T are not drawn between 8 and 10 km, as it was difficult to estimate the vertical velocity spectrum due to reduced detectability of the signal in this height interval on 21 July 1999. The difference in height characteristics of N^2 and temperature during two winter and monsoon days shows distinct features. The temperature profiles for two winter days presented here, show that height as well as the temper-

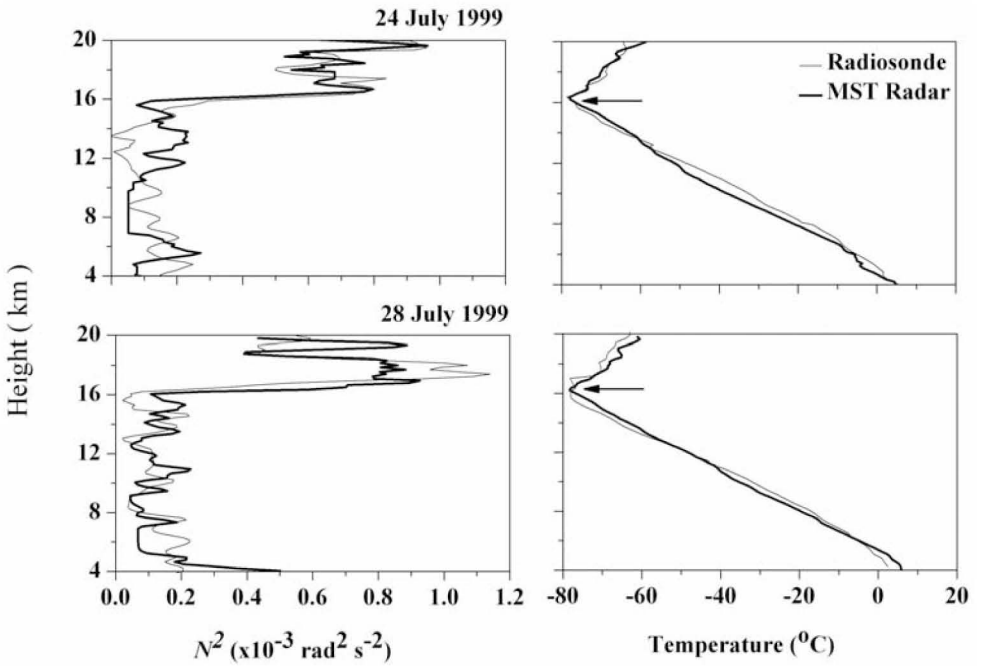

Figure 2. Height profiles of stability parameter (N^2) and atmospheric temperature for two days (24 and 28 July 1999) during monsoon season using radar and radiosonde observations. The horizontal arrows indicate the cold-point tropopause height.

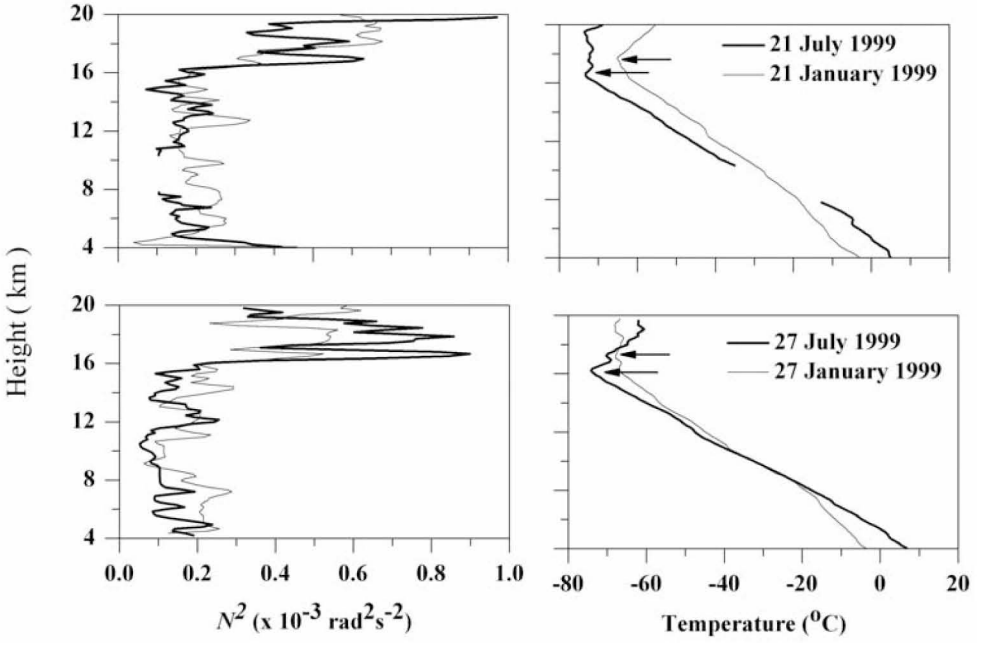

Figure 3. Height profiles of stability parameter (N^2) and atmospheric temperature for two days of monsoon (21 and 27 July 1999) and two days of winter (21 and 27 January 1999) seasons using radar observations. The horizontal arrows indicate the cold-point tropopause height.

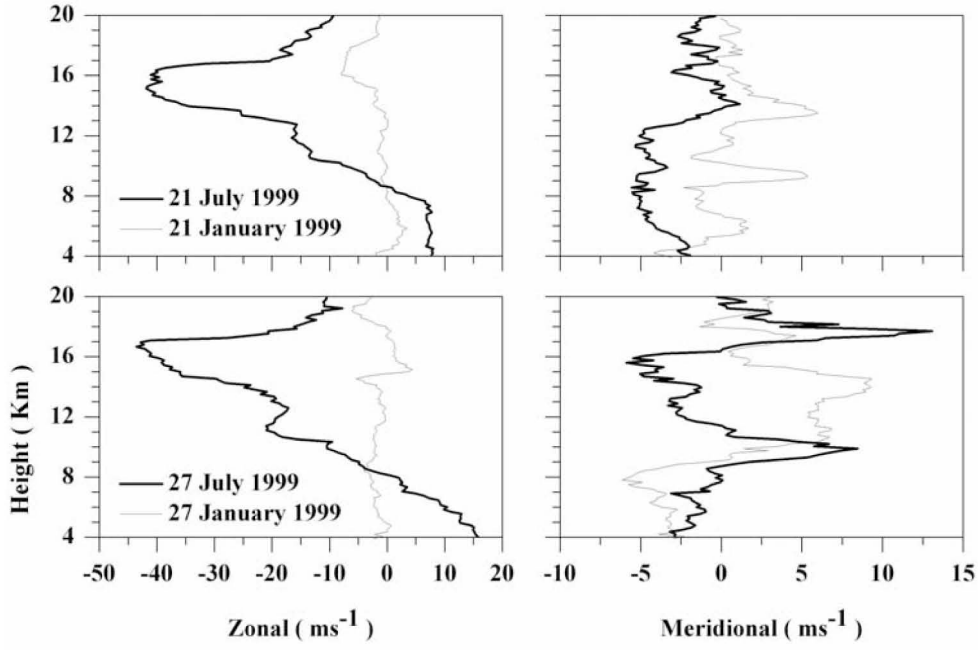

Figure 4. Height profiles of zonal and meridional wind speed for two days of monsoon (21 and 27 July 1999) and winter (21 and 27 January 1999) seasons radar observations.

ature at tropopause (indicated by horizontal arrows) is higher as compared to the two monsoon season days. Figure 3 also shows that the lapse rate during monsoon season tends to be higher as compared to the winter season. Height profiles of atmospheric stability parameter N^2 show that during monsoon season atmosphere is less stable as compared to the winter season, indicating more turbulent activity during monsoon season, as expected.

[18] It is often observed in the lower stratosphere the presence of multiple layer structures in both temperature profile as well as in the radar return, which is attributed due to the propagation or breaking of gravity wave. These temperature structures are known as temperature sheets, i.e., multiple stable layers, which are clearly observed as enhanced N^2 in the lower stratosphere (namely, strong temperature gradient in the upper troposphere and lower stratosphere). Thus, the observed multiple enhanced peaks in the height profile of N^2 are due to the presence of temperature sheets in the lower stratosphere during monsoon [*Luce et al.*, 2001, and references therein]. As we know that during monsoon, the probabilities for the generation of gravity waves are more due to convection, thus, the probabilities of multiple layer in lower stratosphere is also more. However, the lower enhanced peak is due to the temperature gradient at tropopause height.

5.2. Height Profiles of Wind Speed and Vertical Shear During Monsoon and Winter Seasons

[19] Figure 4 shows the height profiles of zonal and meridional wind speed for two days of monsoon and winter seasons. From Figure 4, strong easterly jet winds are observed during monsoon, whereas relatively weaker westerly winds prevail during winter season. Figure 5 shows the height profiles of wind speed and vertical shear of horizontal wind for two days of observations during monsoon and winter seasons. Since the radar resolution is 150 m, the wind shear is calculated with a height resolution of 300 m. From Figures 4 and 5 it can be seen that tropical easterly jet (TEJ) associated winds are observed during monsoon season and strong vertical shears are observed at the upper edge of tropical easterly jet winds during this season. Shears are relatively weaker near the bottom of the jet stream. During the winter season, wind speeds are relative weaker, as compared to monsoon season, and shears are also relatively weak except at some heights.

5.3. Mean Height Profiles of Atmospheric Temperature, Stability Parameter, Wind Speed, and Shear During Monsoon and Winter Seasons

[20] Figure 6 (top) shows the mean height profiles of stability parameter and temperature, and Figure 6

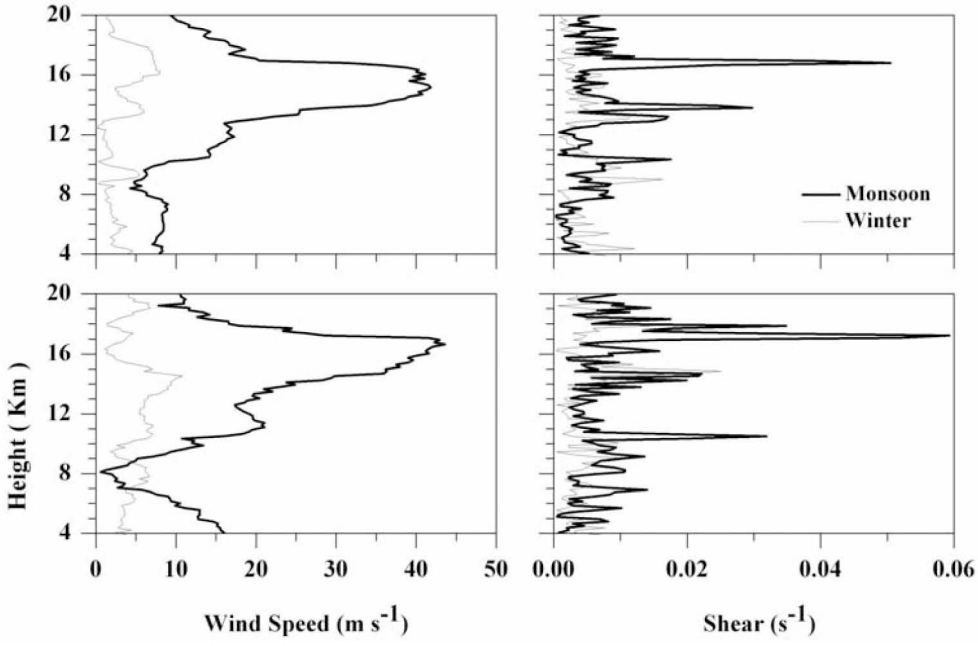

Figure 5. Height profiles of wind speed and vertical shear of horizontal winds for two days of monsoon (21 and 27 July 1999) and two days of winter (21 and 27 January 1999) seasons from radar observations.

(bottom) shows the mean wind speed and vertical shear of horizontal winds obtained using all the individual days of observations for both the seasons. These height profiles are representative of temperature, stability parameter, wind speed and wind shear for monsoon and winter season at this tropical station Gadanki. The horizontal bars show the standard deviation, representing day-to-day variability of these parameters during two observation campaign periods. The average temperature profiles show that during winter season tropopause height is higher where as tropopause temperature is lower as compare to the monsoon season [*Murthy et al.*, 1986]. This particular feature is also observed from atmospheric model by *Sasi and Sen Gupta* [1986] which is applicable to Indian tropical latitudes. The stability parameter N^2 show that during winter season atmosphere is more stable compared to monsoon season and temperature lapse rate is higher during monsoon as compared to winter. One additional distinct feature that can be noticed in Figure 6 is sharp increases in parameter N^2 near the height of tropopause during monsoon season, which is attributed due to the presence of temperature sheets [*Luce et al.*, 2001].

[21] The average profiles of wind speed and shear shows that during monsoon season wind speed as well as shears are high as compared to winter season except at the height 14.5 to 16 km where shear is higher during winter season. This is expected, since peak easterly jet winds are observed during monsoon season in this height range (14.5–16 km) and vertical shears at the core of jet winds are normally weak [see *Ghosh et al.*, 2000].

5.4. Turbulence Parameters During Monsoon and Winter Seasons

[22] Figure 7 shows the height profiles of log ε, log K_h, l_0 and L_B for two days of monsoon and two days of winter seasons, making use of corrected spectral width ($\sigma_{1/2sc}$) and spectral width method 1. It can be noted from Figure 7 that the height profiles of monsoon season ε and K_h show higher values as compared to winter season except in the height range of 15.15–15.90 km. In Figures 7 and 8, height profiles of various turbulence parameters are not drawn during monsoon season in the height range of 14.55–15 km, as it is difficult to estimate the spectral width $\sigma_{1/2obs}$ accurately in this height range due to reduced detectability of the signal in this height interval. Height profiles of turbulence parameters of both the seasons show multiple peaks in the height range of 16–20 km as well as at the lower heights. These peaks are more distinct during monsoon season as compared to winter season. The inner scale size l_0 during monsoon season is less compared to winter season as it is inversely proportional to the ε. The increasing trend of inner scale size l_0 with height is due to decreasing air density. The buoyancy scale size L_B, above 5 km, is higher during the

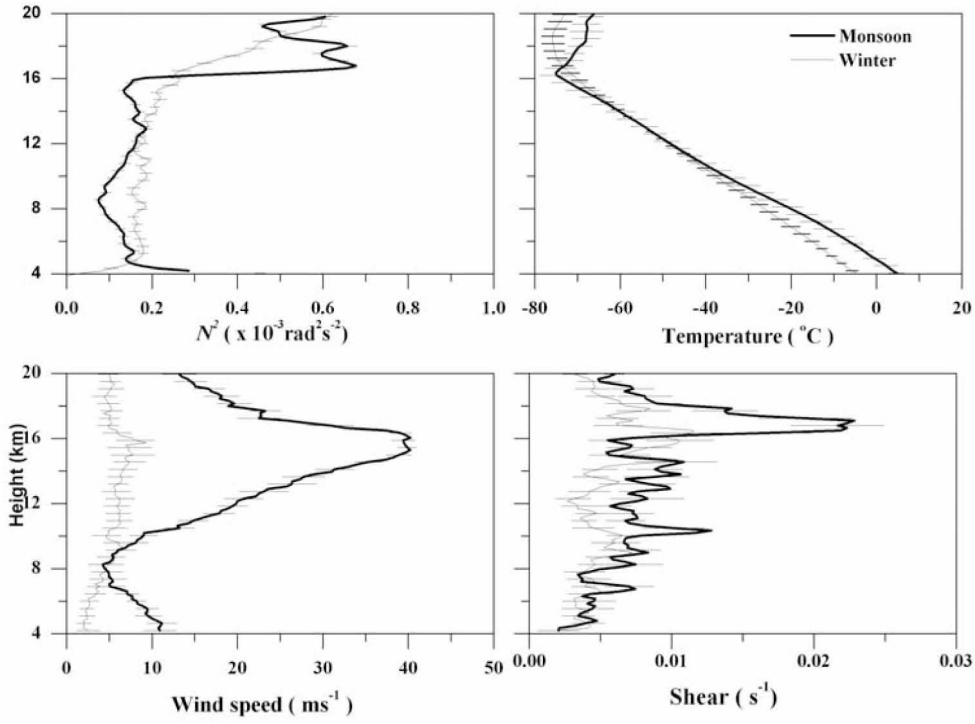

Figure 6. Height profiles of (top) mean atmospheric stability parameter and temperature, and (bottom) wind speed and vertical shear of horizontal winds for monsoon and winter seasons. Horizontal bars show the standard deviation of measurements for each season.

monsoon season as compared to winter season and afterwards the value is decreasing with height.

[23] Figure 8 shows mean height profiles of log ε, log K_h, l_0, and L_B obtained using the data of all the individual days during monsoon and winter seasons. These height profiles represent the height variation of the turbulence parameters at this tropical station Gadanki during monsoon and winter seasons. It is clearly noted that the value of eddy dissipation rate ε during monsoon season is larger in lower altitudes up to ~14 km and the minimum value is found at about 2–2.5 km below the mean tropopause height as compared to winter. The maximum eddy dissipation rate ε during monsoon is found in the lower stratosphere, above the height of jet stream where strong wind shear is observed. This shows an abrupt transition of eddy dissipation rate ε across the tropopause. It is noteworthy that the maximum wind shear and enhanced stability parameter N^2 occurs in the vicinity of mean tropopause height during monsoon. Thus, the secondary peak of ε during monsoon is attributed due to the existence of strong wind shear and enhanced stability parameter N^2 in the vicinity of mean tropopause height. During winter such secondary peak is not observed which may be due to the absence of strong wind shear or stability parameter N^2. However, in the vicinity of mean tropopause height, there is no remarkable variation in eddy dissipation rate between winter and monsoon. Thus, the larger difference of eddy dissipation rate ε between monsoon and winter is due to the seasonal changes of $(\sigma_{1/2})^2$ and N^2. In lower height region below tropopause, the values of ε mainly contributed by $(\sigma_{1/2})^2$, whereas above tropopause it will be the contribution by both $(\sigma_{1/2})^2$ and N^2. This is in consistence with the results obtained by *Nastrom and Eaton* [1997a].

[24] *Rao et al.* [2001] have reported the diurnal variability of turbulence parameters at Gadanki. The authors found that peak value of eddy dissipation rate ε occurs between 1700 and 1900 h (IST) in both monsoon and winter. It is noteworthy that the present observation is between 1645 to 1730 IST in mode 1 experiment and 1730 to 1930 IST mode 2 experiment. Since the observations time in both the seasons remain same (1630–1930), thus in the present study diurnal effect is ignored.

[25] The height profile of K_h clearly show that monsoon season K_h values are higher compared to the winter season. In monsoon season K_h generally has maximum values at lower altitudes, i.e., 4–13.5 km and a secondary peak is observed in the vicinity of tropopause with a minimum in the height of occurrence of maximum intensity of jet stream. Values of K_h in winter season in

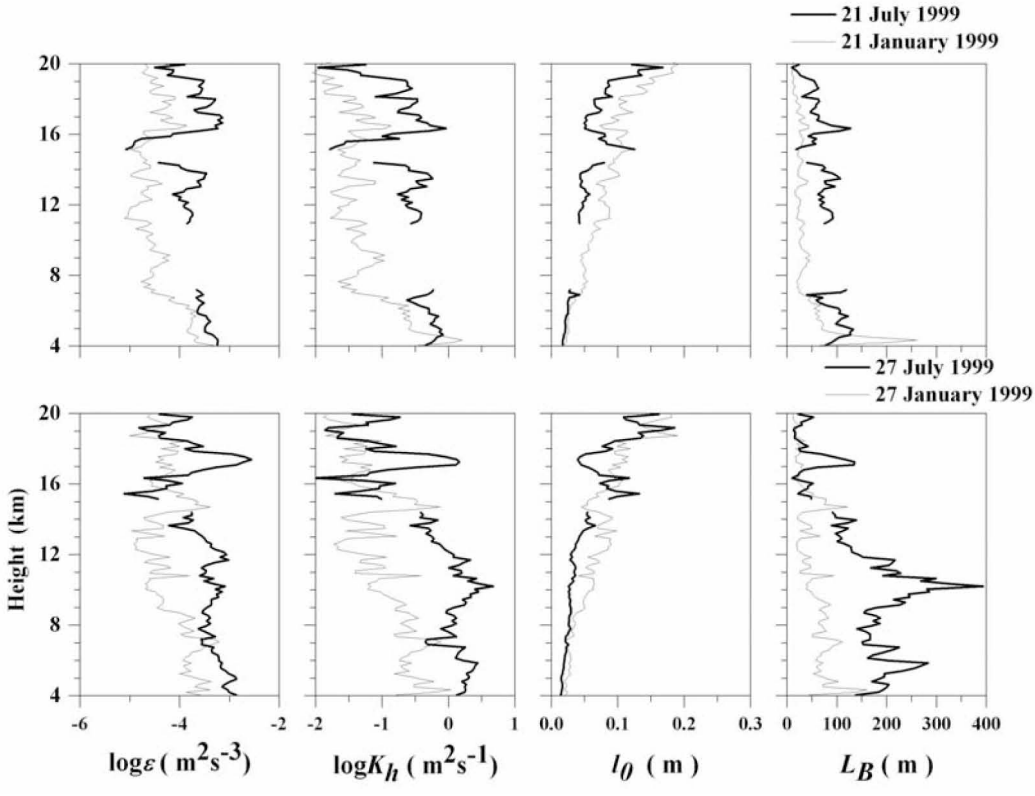

Figure 7. Height profiles of the eddy dissipation rate (ε), vertical eddy diffusivity (K_h), inner scale size (l_0), and buoyancy scale size (L_B) for two days of monsoon (21 and 27 July 1999) and two days of winter (21 and 27 January 1999) seasons.

the altitude range of 15–15.5 km are slightly larger than monsoon season values. This is again accredited due to less wind shear at the core of the jet stream during monsoon. The height profiles of inner scale size l_0 in the lower altitude, i.e., 4–12 km show an increase with height for both the seasons. The values of both the season are comparable except in the upper troposphere and lower stratosphere where winter season values are higher. The height profiles of Buoyancy scale size L_B of turbulence shows the values decrease with height for both the seasons but above jet stream, the values are almost constant. In comparison to winter, monsoon season values are larger between 5 and 14.55 km with a peak between 9 and 13 km. The height profiles of l_0 and L_B show that inertial subrange decreases with increase in height for both seasons.

6. Discussion

[26] The height profiles characteristics of turbulence parameters during both the seasons are almost similar but magnitudes during monsoon are higher in general, as compared to winter season. Higher values of turbulence parameters at lower and middle troposphere during monsoon season partly may be due to higher values of wind shear (see Figure 5, bottom). Enhanced values of turbulence parameters in upper troposphere and lower stratosphere are due to strong observed vertical shear of horizontal winds and temperature gradients associated to sharp enhancement in N^2 (see Figure 6) during monsoon season at these heights. During winter season, turbulence parameters are observed to be higher compared to monsoon season in the vicinity of tropical tropopause. Normally peak jet winds are observed during monsoon season at the height region between 14 and 17 km (near tropopause). At the core jet winds, the vertical shears of horizontal winds are small. So, in this region turbulence parameters can be expected to be weaker during monsoon season as compared to winter season. At the lower stratospheric height, i.e., above the jet stream (>19 km), during both the season winds, vertical shears of horizontal winds and temperature gradients are same. In lower stratospheric region above the height level of

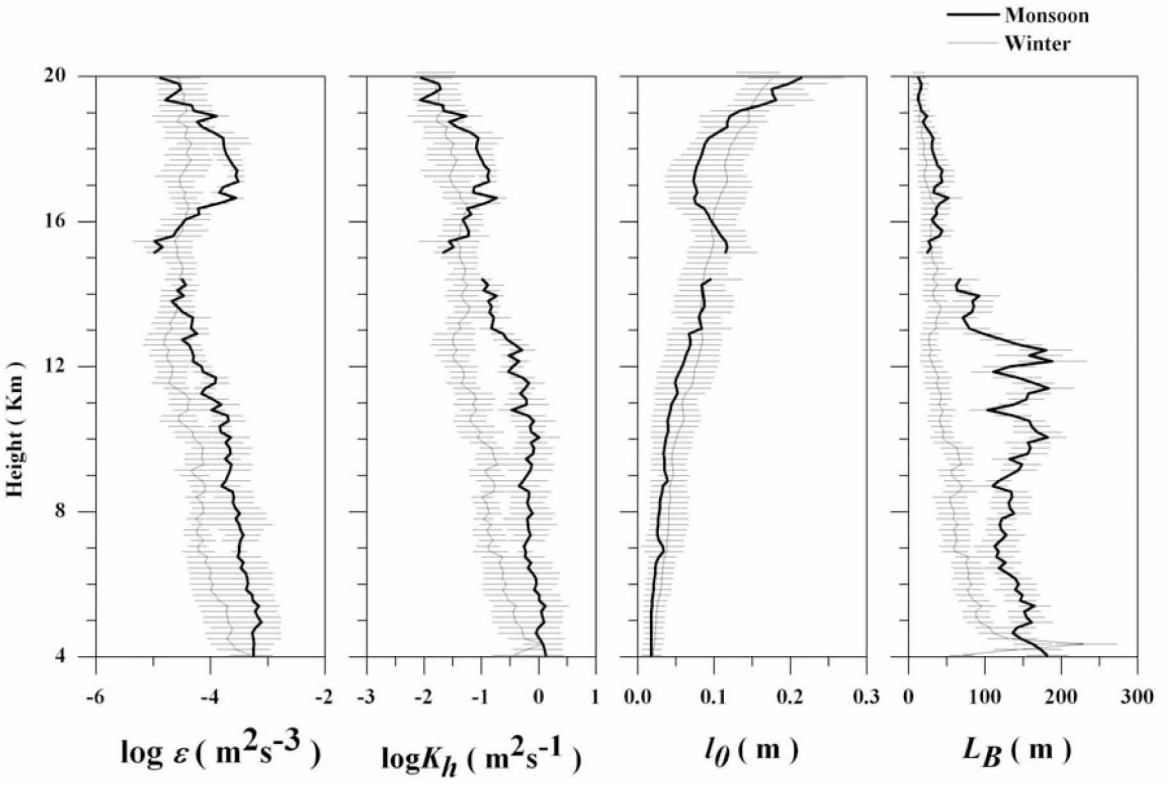

Figure 8. Mean height profiles of ε, K_h, l_0, and L_B using the corrected spectral width of all the data from campaigns of observations from 19 July to 14 August during monsoon season and 19 January to 10 February 1999 during winter season.

19 km, turbulence parameters are almost equal in magnitude during both the seasons as expected.

[27] It would be interesting to compare height characteristics of various turbulence parameters and their magnitudes with some of the available observations. *Sato and Woodman* [1982], from Arecibo radar (18°N) measurement on one winter day and reported a value of ε between 10^{-5} to 10^{-3} m^2s^{-3} in the height range of 14–19 km with a minimum value at a height of 17.4 km. The corresponding values for K_h, reported by these authors, are in the range of 0.01 to 1.0 with a minimum value at 17.4 km. The corresponding values from the present set of measurements for the same height range are of the same order as reported by *Sato and Woodman* [1982]. *Jain et al.* [1995] reported measurements of turbulence parameters using spectral width methods for Gadanki, in the height range of 4–11 km using Indian MST radar in ST mode. These measurements refer to one day in March. The magnitudes of ε, K_h, and L_B reported by *Jain et al.* [1995] compare well with the present monsoon season measurements. *Satheesan and Murthy* [2002] reported measurements of turbulence parameter ε for Gadanki during winter season (January–February) in the height range of 3.6–25 km using Indian MST radar observations. This parameter is estimated by spectral width, power and variance methods and the values obtained using these methods are compared. These measurements compare well with the winter season measurement magnitudes as well as characteristics wise reported in the present study. A comparison of the present measurements of ε with those reported by *Rao et al.* [1997], using spectral width method, for Gadanki for the month of July 1996, shows similarity in height structure. However, magnitudes obtained from present measurements are significantly higher than those reported by *Rao et al.* [1997].

[28] *Fukao et al.* [1994] presented three years of measurements of K_h using MU radar. *Nastrom and Eaton* [1997b] have presented climatology of K_h at White Sand Missile Range (WSMR) during 1991–1995. *Nastrom and Eaton* [1997a] also presented detailed climatology of ε using WSMR for the period 1991–1995. The authors found that the maximum eddy dissipation rate at the lower altitude and the minimum values at about 2–3 km

below the tropopause height, depending upon seasons. They have also reported that summer values are several decibels larger than the winter value in the middle troposphere. The largest seasonal difference of eddy dissipation rate ε are explained in term of seasonal changes of $(\sigma_{1/2})^2$ and N^2. Their studies also show the transition of ε across the tropopause with maximum at lower stratosphere in all seasons. However, there is no much remarkable seasonal variation in the vicinity of tropopause. These measurements reported in these papers also make use of the spectral width method but refer to midlatitudes.

[29] *Rao et al.* [2001] and *Ghosh et al.* [2003] have shown the value of K_h in the range of 0–0.8 m^2 s^{-1} using Gadanki MST radar. The present observation of Kh is well comparable with the value reported earlier at Gadanki. The value of K_h reported by *Fukao et al.* [1994] and *Kurosaki et al.* [1996] for the month of July is in the range of 0.3–3.0 with a peak value at around 12 km. The corresponding value given by *Nastrom and Eaton* [1997b] is also in the same range but the height structure of the profile in two cases is different. However, the value of K_h at Gadanki above 14 km is somewhat smaller (0.01–0.3 m^2s^{-1}) as compared to those reported by *Fukao et al.* [1994] and *Nastrom and Eaton* [1997b]. This may be due to the latitudinal difference, as the present observations are over tropical station Gadanki, whereas the observations made by *Fukao et al.* [1994] and *Nastrom and Eaton* [1997b] are over midlatitude. The height structures of K_h show a secondary peak in the vicinity of tropopause. This height structure of K_h is similar to that reported by *Nastrom and Eaton* [1997b]. The height profile of ε as reported by *Nastrom and Eaton* [1997a] for the month of July for WSMR is very similar to present monsoon season observations and comparable in magnitude. Both of these results show a secondary peak in the vicinity of tropopause. Further studies at this latitude will be aimed to quantify the seasonal climatology of turbulence parameters by collecting long-term MST radar data in mode 1 followed by mode 2 experiments.

7. Conclusions

[30] In the present analysis, observations made in two intensive campaigns carried out over Gadanki using MST radar are used for the estimation of turbulence parameters in two different seasons. The following salient features are brought out.

[31] 1. MST radar and radiosonde observations of temperature and Brunt-Vaisala frequency are reasonably well matched during monsoon season for convection free days.

[32] 2. During monsoon season strong easterly jet winds are observed, where as during winter season weak westerly winds are observed. During monsoon season horizontal winds as well as vertical shear of horizontal winds are stronger as compared to winter season.

[33] 3. During winter season, tropopause height is higher, whereas tropopause temperature is lower as compared to monsoon season. This phenomenon is also confirmed by atmospheric model, a representative of Indian tropical region.

[34] 4. It is clear from the present observations that monsoon season turbulence parameters magnitudes are higher as compared to winter season except in the height region of 13.5–16 km., which is the jet core region. The higher values of turbulence parameters, at other height, during monsoon season are due to large contribution from strong vertical shear of horizontal winds and temperature gradient during this season.

[35] **Acknowledgments.** The authors would like to thank the scientific and technical staff of NARL, Gadanki, who have contributed to the collection of data reported in this paper. Thanks are also due to the India Meteorological Department (IMD) for successfully conducting the radiosonde campaign from NARL during the July–August 1999 period. The authors would like to sincerely thank B. V. Krishna Murthy for his valuable discussions and suggestions. The authors gratefully acknowledge all three reviewers for their valuable comments and suggestions which considerably improved the manuscript.

References

Atlas, D., R. C. Srevastava, and P. W. Sloss (1969), Wind shear and reflectivity gradient effects on Doppler radar spectra, II, *J. Appl. Meteorol.*, *8*, 384–388.

Cohn, S. A. (1995), Radar measurements of turbulent eddy dissipation rate in the troposphere: A comparison of techniques, *J. Atmos. Oceanic Technol.*, *12*, 85–95.

Cunnold, D. M. (1975), Vertical transport coefficients in the mesosphere obtained from radar observations, *J. Atmos. Sci.*, *32*, 2191–2199.

Das, S. S., A. R. Jain, K. K. Kumar, and D. N. Rao (2008), Diurnal variability of the tropical tropopause: Significance of VHF radar measurements, *Radio Sci.*, *43*, RS6003, doi:10.1029/2008RS003824.

Fukao, S., M. D. Yamanaka, A. Naoki, W. K. Hocking, T. Sato, M. Yamamoto, T. Nakamura, T. Tsuda, and S. Kato (1994), Seasonal variability of vertical eddy diffusivity in the middle atmosphere: 1. Three-year observations by the middle and upper atmosphere radar, *J. Geophys. Res.*, *99*, 18,973–18,987.

Gage, K. S., and B. B. Balsley (1980), On the scattering and reflection mechanisms contributing to clear air radar echoes from the troposphere, stratosphere, and mesosphere, *Radio Sci.*, *15*(2), 243–257.

Gage, K. S., J. L. Green, and T. E. Vanzandt (1980), Use of Doppler radar for the measurement of atmospheric turbulence parameters from the intensity of clear air echoes, *Radio Sci.*, *15*, 407–416.

Ghosh, A. K., A. R. Jain, and V. Sivakumar (2000), Characteristics of atmospheric wind, associated shear and turbulence: Indian MST radar measurement during summer monsoon season, Indian *J. Radio Space Phys.*, *29*, 222–230.

Ghosh, A. K., V. Sivakumar, K. K. Kumar, and A. R. Jain (2001), VHF radar observations of atmospheric winds, associated shears and C_n^2 at a tropical location: Interdependence and seasonal pattern, *Ann. Geophys.*, *19*, 965–973.

Ghosh, A. K., A. R. Jain, and V. Sivakumar (2003), Simultaneous MST radar and radiosonde measurements at Gadanki (13.5°N, 79.2°E): 2. Determination of various turbulence parameters, *Radio Sci.*, *38*(1), 1014, doi:10.1029/2000RS002528.

Hocking, W. K. (1983), On the extraction of atmospheric turbulence parameters from radar backscatter Doppler spectra I, Theory, *J. Atmos. Terr. Phys.*, *45*, 89–102.

Hocking, W. K. (1985), Measurements of turbulent energy dissipation rates in the middle atmosphere by radar techniques: A review, *Radio Sci.*, *20*, 1403–1422.

Hocking, W. K. (1986), Observation and measurements of turbulence in the middle atmosphere with a VHF radar, *J. Atmos. Terr. Phys.*, *48*, 655–670.

Hocking, W. K. (1996), An assessment of the capabilities and limitations of radars in measurements of upper atmospheric turbulence, *Adv. Space Res.*, *17*, 3–47.

Hocking, W. K., and K. Lawry (1989), Radar measurements of atmospheric turbulence intensities by both C_n^2 and spectral width methods, *IMAP Handb.*, *28*.

Jain, A. R., Y. J. Rao, P. B. Rao, G. Viswantathan, S. H. Damle, P. Balamuralidhar, and A. Kulkarni (1994), Preliminary observations using ST mode of the Indian MST radar: Detecting the signature of the tropopause, *J. Atmos. Terr. Phys.*, *56*, 1157–1162.

Jain, A. R., Y. J. Rao, P. B. Rao, V. K. Anandan, S. H. Damle, P. Balamuralidhar, A. Kulakerni, and G. Viswanathan (1995), Indian MST radar: 2. First scientific results in ST mode, *Radio Sci.*, *30*, 1139–1158.

Jain, A. R., S. S. Das, T. K. Mandal, and A. P. Mitra (2006), Observations of extremely low tropopause temperature over Indian tropical region during monsoon and post monsoon months: Possible implications, *J. Geophys. Res.*, *111*, D07106, doi:10.1029/2005JD005850.

Kurosaki, S., M. D. Yamanaka, H. Hashiguchi, T. Sato, and S. Fukao (1996), Vertical eddy diffusivity in the lower and middle atmosphere: A climatology based on the MU radar observations during 1986–1992, *J. Atmos. Terr. Phys.*, *58*, 727–734.

Lilly, D. K., D. E. Waco, and S. I. Adelfang (1974), Stratospheric mixing estimated from high-altitude turbulence measurements, *J. Appl. Meteorol.*, *13*, 488–493.

Luce, H., M. Crochet, and F. Dalaudier (2001), Temperature sheets and aspect sensitive radar echoes, *Ann. Geophys.*, *19*, 899–920.

Murphy, D. J., W. K. Hocking, and D. C. Fritts (1994), An assessment of the effect of gravity waves on the width of radar Doppler spectra, *J. Atmos. Terr. Phys.*, *56*, 17–29.

Murthy, B. V. K., K. Parameswaran, and K. O. Rose (1986), Temporal variations of the tropical tropopause characteristics, *J. Atmos. Sci.*, *43*, 914–922.

Nastrom, G. D., and F. D. Eaton (1997a), Turbulence eddy dissipation rates from radar observations at 5–20 km at White Sand Missile Range, New Mexico, *J. Geophys. Res.*, *102*, 19,495–19,506.

Nastrom, G. D., and F. D. Eaton (1997b), A brief climatology of eddy diffusivities over White Sand Missile Range, New Mexico, *J. Geophys. Res.*, *102*, 29,819–29,826.

Nastrom, G. D., K. S. Gage, and W. L. Ecklund (1986), Variability of turbulence, 4–20 km, in Colorado and Alaska from MST radar observations, *J. Geophys. Res.*, *91*, 6722–6734.

Rao, D. N., P. Kishore, T. Narayana Rao, S. V. B. Rao, K. K. Reddy, M. Yarraiah, and M. Hareesh (1997), Studies on refractivity structure constant, eddy dissipation rate and momentum flux at a tropical latitude, *Radio Sci.*, *32*, 1375–1389.

Rao, D. N., T. Narayana Rao, M. Venkataratnam, S. Thulasiraman, and S. V. B. Rao (2001), Diurnal and seasonal variability of turbulence parameters observed with Indian mesosphere-stratosphere-troposphere radar, *Radio Sci.*, *36*, 1439–1457.

Rao, P. B., A. R. Jain, P. Kishore, P. Balamuralidhar, S. H. Damle, and G. Viswanathan (1995), Indian MST radar: 1. System description and sample vector wind measurements in ST mode, *Radio Sci.*, *30*, 1125–1138.

Rao, T. N., K. N. Uma, D. Narayana Rao, and S. Fukao (2008), Understanding the transportation process of tropospheric air entering the stratosphere from direct vertical air motion measurements over Gadanki and Kototabang, *Geophys. Res. Lett.*, *35*, L15805, doi:10.1029/2008GL034220.

Revathy, K., S. R. Prabhakaran Nair, and B. V. K. Murthy (1996), Deduction of temperature profile from MST Radar observations of vertical wind, *Geophys. Res. Lett.*, *23*, 285.

Revathy, K., S. R. Prabhakaran Nair, and B. V. K. Murthy (1998), Estimation of error in the determination of temperature using MST radar, *Indian J. Radio Space Phys.*, *27*, 241–243.

Rotteger, J. (1986), Determination of Brunt-Vaisala frequency from vertical velocity spectra, *MAP Handb.*, *20*, 1968–1972.

Rotteger, J., and M. F. Larsen (1990), UHF/VHF radar techniques for atmospheric research and wind profiler applications, in *Radar Meteorology*, edited by D. Atlas, pp. 5235–5281, Am. Meteorol. Soc., Boston, Mass.

Sasi, M. N., and K. Sen Gupta (1986), A reference atmosphere for Indian equatorial zone from surface to 80 km–1985, *Sci. Rep. SPL:SR:006:85*, Space Phys. Lab., Vikram Sarabhi Space Cent., Trivandrum, India.

Satheesan, K., and B. V. K. Murthy (2002), Turbulence parameters in tropical troposphere and lower stratosphere, *J. Geophys. Res.*, *107*(D1), 4002, doi:10.1029/2000JD000146.

Sathiyamoorthy, V. (2005), Large scale reduction in the size of the tropical easterly jet, *Geophys. Res. Lett.*, *32*, L14802, doi:10.1029/2005GL022956.

Sato, T., and R. F. Woodman (1982), Fine altitude resolution observations of stratospheric turbulent layers by the Arecibo 430-MHz radar, *J. Atmos. Sci.*, *39*, 2546–2552.

Uma, K. N., and T. N. Rao (2009), Diurnal variation in vertical air motion over a tropical station, Gadanki (13.5°N, 79.2°E), and its effect on the estimation of mean vertical air motion, *J. Geophys. Res.*, *114*, D20106, doi:10.1029/2009JD012560.

Weinstock, J. (1978), On the theory of turbulence in the buoyancy subrange of stratified flows, *J. Atmos. Sci.*, *35*, 634–649.

Weinstock, J. (1981), Vertical turbulence diffusivity for weak or strong stable stratification, *J. Geophys. Res.*, *86*, 9925–9928.

S. S. Das and K. N. Uma, Space Physics Laboratory, Vikram Sarabhai Space Centre, Department of Space, ISRO, Trivandrum 695022, India. (dassiddhu@yahoo.com)

A. K. Ghosh, Meteorology Facility, Satish Dhawan Space Centre, Department of Space, ISRO, Sriharikota 524124, India.

A. R. Jain, Radio and Atmospheric Sciences Division, National Physical Laboratory, CSIR, New Delhi 110012, India.

K. Satheesan, Swedish Institute of Space Physics, Box 812, SE-981 28 Kiruna, Sweden.